Patterns of traveling intrinsic localized modes in a driven electrical lattice

L. Q. English, R. Basu Thakur, and Ryan Stearrett
Department of Physics and Astronomy, Dickinson College, Carlisle, Pennsylvania 17013, USA
(Received 1 February 2008; published 2 June 2008)

The emergence of very stable traveling intrinsic localized modes (ILMs) locked to a uniform driver is demonstrated in a discrete electrical transmission line. The speed of these traveling ILMs is tunable by the driver amplitude and frequency. It is found to be quite sensitive to the ratio of intersite to on-site nonlinearity. The number of traveling ILMs can also be selected via the driving conditions and appears to be the result of a spatiotemporal pattern selection process.

DOI: 10.1103/PhysRevE.77.066601 PACS number(s): 05.45.Yv, 63.20.Pw, 47.54.De

I. INTRODUCTION

Solitons and kinks of well-defined, nonzero velocities constitute the quintessential nonlinear excitations in continuous media. It is well-known that in the continuum limit, one general feature of localized excitations is that they travel [1]. In discrete lattices, the situation is reversed; here, the discrete soliton, better known as an intrinsic localized mode (ILM) or discrete breather (DB) tends to be stationary in most circumstances. This is not surprising, since in the anticontinuous limit [2], of course, all excitations must become pinned.

One technique by which a stationary ILM can be made to move [3,4] involves perturbing the stable (odd-parity) localized eigenvector. Then the instability associated with an antisymmetric perturbation was shown to depin the ILM, causing it either to move slowly through the lattice or to hop between neighboring sites.

In another approach, moving ILMs were constructed in an anharmonic lattice by considering an envelope on top of a particular plane-wave mode [5–7], and numerical simulations revealed that they were long-lived. Similarly, in spin systems moving ILMs were initiated via the modulational instability of a plane-wave mode inside the dispersion curve [8], but here they were found numerically to quickly slow down and become trapped at a given lattice site. Most recently, traveling ILMs have been experimentally generated in a micromechanical system [9]. Nevertheless, studies of traveling ILMs have remained sparse in the literature.

This paper builds on the earlier work of Ref. [10], but now discusses the experimental generation of slowly traveling ILMs that are locked to a uniform driver, with an emphasis on characterizing these modes and their speeds through the lattice as a function of driver amplitude and frequency. These slowly propagating ILMs which are produced by a spatially homogenous driver are different from the broader, fast-moving envelope solitons also seen in this lattice when a pulse is injected at either end of an undriven line circuit [11,12]. Compared to the envelope soliton [11], the ILM is narrower by roughly one order of magnitude (24 cells versus 2.5 cells), the speed is lower by at least two orders of magnitudes (2500 cell/ms versus 20 cell/ms), and the ILM wings do not approach zero amplitude due to the presence of the driver at each cell.

Furthermore, in contrast to the earlier studies on envelope solitons, the ILMs emerge spontaneously rather than being seeded by a pulse. We find that no direction of travel through the ring lattice is preferred, but once the direction is chosen, the ILM can continue for as long as the driver persists. We have empirically mapped out certain regions of driver amplitude and frequency which were found to sustain the traveling ILMs indefinitely.

In the system studied here, in which the intersite nonlinearity is of the same order as the on-site nonlinearity, these traveling modes are the generic nonlinear excitations. No sophisticated driving scheme has to be employed in order to excite these traveling modes. In contrast to the recent experimental studies on micromechanical cantilever arrays [9], where traveling ILMs were observed when starting the driver between two plane-wave frequencies and then chirping it into a nonlinear region, the traveling ILMs here are simply obtained with a fixed-frequency driver. Their speed is found to depend strongly on the driver amplitude and it is sensitive to the ratio of on- and inter-site nonlinearity.

The number of localized features within the lattice can also be selected via the driving conditions. Patterns with up to five ILMs within a 24-node lattice were stabilized. More complex patterns with noninteger numbers of ILMs can also be generated.

II. EXPERIMENT

The experimental system-*a* bi-inductive discrete electrical transmission line was described in some detail in Ref. [10]. Following the approach in Ref. [13], the capacitance of the nonlinear diode is approximated as $C(V)=C_0\exp(-\alpha V)$, where C_0 is roughly 800 pF for the diodes used here. The system is driven at each node via large resistors (10 kΩ). Thus each unit cell contains an in-line inductor, L_1, a diode of variable capacitance to ground, second inductor, L_2, to ground, and a resistor connected to the driving signal. Expanding the logarithmic expression for voltage as a function of charge to third order as in Ref. [13], we arrive at the following set of differential equations governing the lattice:

$$\frac{d^2Q_n}{dt^2}+\left(\omega_0^2Q_n-\frac{\omega_0^2}{2Q_0}Q_n^2+\frac{\omega_0^2}{3Q_0^2}Q_n^3\right)+\omega_1^2(2Q_n-Q_{n+1}-Q_{n-1})$$
$$-\frac{\omega_1^2}{2Q_0}(2Q_n^2-Q_{n+1}^2-Q_{n-1}^2)+\frac{\omega_1^2}{3Q_0^2}(2Q_n^3-Q_{n+1}^3-Q_{n-1}^3)$$
$$+\frac{1}{RC_0}\left[1-\left(\frac{Q_n}{Q_0}\right)+\left(\frac{Q_n}{Q_0}\right)^2\right]\frac{dQ_n}{dt}=\frac{1}{R}\frac{dV_d}{dt}. \quad (1)$$

Here $\omega_0=\sqrt{1/L_2C_0}$, $\omega_1=\sqrt{1/L_1C_0}$, and $Q_0=C_0/\alpha$.

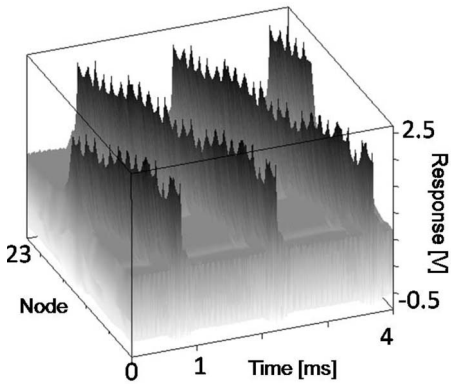

FIG. 1. Surface plot of the voltage response in space and time depicting one ILM completing three "laps" around the ring lattice.

Soft nonlinearity results from the quadratic terms, and these dominate the cubic terms (hard nonlinearity) for the amplitudes attained in this study. Furthermore, Eq. (1) contains both on-site nonlinear terms as well as an intersite nonlinear term. Their ratio is evaluated as

$$\frac{\text{intersite}}{\text{on-site}} = \left(\frac{\omega_1}{\omega_0}\right)^2 = \frac{L_2}{L_1}. \tag{2}$$

Therefore this ratio is controlled only by the inductance values of the in-line inductor, L_1, and the inductor to ground, L_2. In this study, $L_1=680\ \mu$H and $L_2=330\ \mu$H. In order to test for a dependence on the ratio in Eq. (2), we also show data for $L_2=150\ \mu$H toward the end of the paper. Note that Eq. (1) contains a damping term due to the 10 kΩ resistors used to couple the driving signal to the lattice; in fact, $1/RC_0 \approx 1/15\omega_0$. Another source of damping not accounted for in Eq. (1) derives from the ohmic resistance of the inductors, which is around 2Ω.

As in Ref. [10], the lattice is arranged in the shape of a ring, so as to eliminate boundaries. The ring lattice consists of 24 nodes each of which is monitored by a fast analog-to-digital converter. Since simultaneous sampling at each node is essential, three eight-channel digitizing cards of 3 MSPS throughput were synchronized to the same time-base and triggered simultaneously. The data was then streamed to a computer equipped with a PCIe interface card. The ring lattice was driven uniformly using a digital signal generator with pulse modulation capabilities, as well as frequency key shifting (FSK).

III. RESULTS AND DISCUSSION

The basic phenomenon of traveling ILMs locked to the driver is easily obtained in this system. Figure 1 illustrates a typical voltage response at each node as a function of time. A sharply localized feature is clearly seen to travel through the lattice. Since the lattice loops back on itself, the localized mode emerges at the opposite end of the lattice immediately after leaving it at one end. It should be noted that Fig. 1 represents the steady-state response of the system to a driver that was switched on a very long time prior to this measurement. The surface plot reveals ridges along the trajectory of the ILM as it transitions from one node to the next. Here the amplitude of the driver was set at 1.5 V and the frequency at 288 kHz.

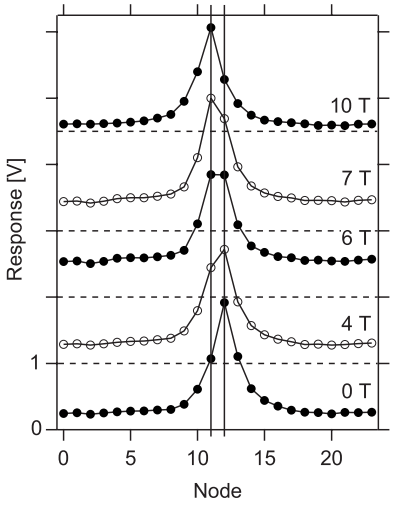

FIG. 2. Detailed look at the ILM transition from one node to the next. Note that this site-hopping occurs over many periods, T.

It is straightforward to show that the ILM center maintains a constant phase relationship with the driver. In fact, the nodes in the wings of the ILM are 90° out of phase in voltage. Since according to Eq. (1) the driving term appears in the form of the first derivative of the driver voltage V_d, it follows that the ILM wings respond in phase with the driving term. This conclusion would be expected for a driver set below the uniform mode in a system with soft nonlinearity, and it is also in agreement with results recently reported for ILMs in a system of coupled pendulums [14]. For lower driving amplitudes, the ILM center is somewhat less than 90° out of phase with the driving term, but this phase difference decreases with larger driver amplitude.

Let us examine the transition from one node to the next more closely. Figure 2 shows traces of the traveling ILM at five different times separated by multiples of the ILM period (labeled T in the figure). The lowest trace shows the ILM centered on node 12, and in the uppermost trace the ILM has fully moved to node 11 after ten complete ILM oscillations. The intermediate traces depict the ILM in transition.

We observe that after about four periods a noticeable asymmetry develops in the ILM profile, and after six periods the two neighboring nodes are at equal amplitude. Incidentally, this progression explains the ridges seen in Fig. 1. The ILM attains its largest amplitude when it is momentarily centered on one particular node and a minimum amplitude when it is centered on two neighboring nodes. The ILM-wing amplitude is seen to vary somewhat over the course of one hopping cycle.

It should be pointed out that the duration of the transition from one node to the next is not a precise constant of the motion. Thus on a fine time scale the hopping speed can vary noticeably perhaps due to small random fluctuations in component properties. Nevertheless, on a larger scale, the ILM speed is constant to remarkable precision and reproducibility.

The question now arises as to the driving conditions that can sustain the traveling ILM. Figure 3(a) depicts the empiri-

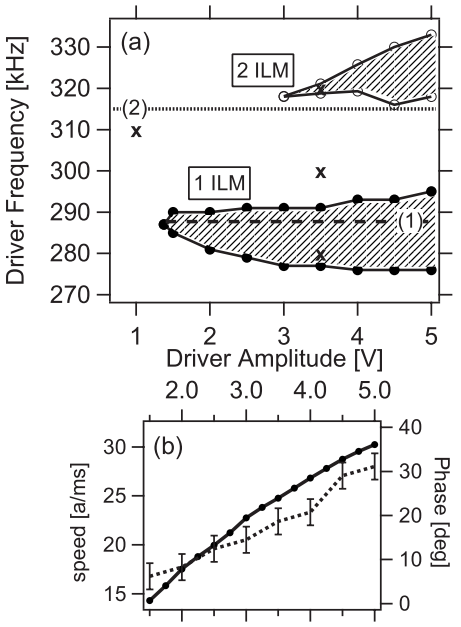

FIG. 3. (a) Hatched regions indicate driving conditions which lead to stable moving ILMs. The dotted line (2) indicates the bottom of the linear dispersion curve. (b) ILM speed (solid, left axis) and phase difference between driver and ILM center (dotted, right axis) versus driver amplitude along the dashed line (1) in (a).

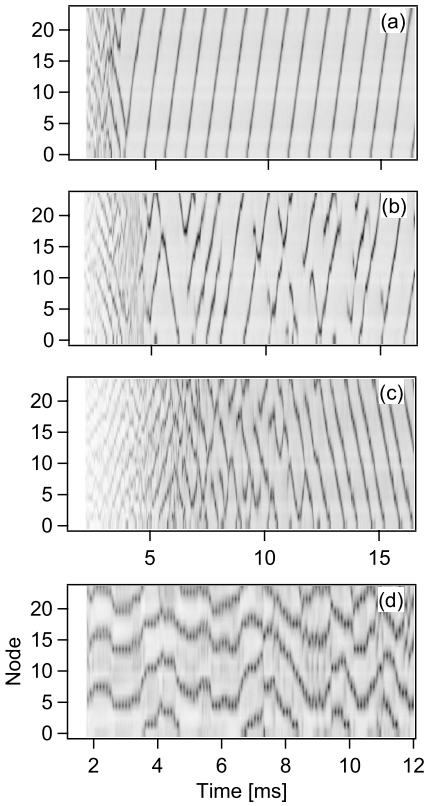

FIG. 4. The energy density plots corresponding to four different driving conditions are shown. (a)–(c) are for an amplitude of 3.5 V and show the transition from one to two traveling ILMs, whereas for (d) the driver amplitude was lowered to 1 V.

cal regions for which locked ILMs were obtained. The axes are driver amplitude and frequency, and the hatched areas indicate regions in this parameter space where stable locked patterns of localized modes are produced. In the lower region, the resultant pattern is formed simply by one traveling ILM. The threshold driver amplitude is about 1.4 V; here the frequency has to be precisely tuned to 288 kHz. As the driver amplitude is increased, a band of frequencies opens up. At an amplitude of 5 V, the frequency can be set as low as 276 kHz and as high as 296 KHz—a range of 20 kHz.

A second region is observed at somewhat higher frequencies in which the driver locks on to two ILMs moving side by side. The amplitude threshold for this pattern is close to 3 V and thus roughly twice that of the lower band. Interestingly, this region falls above the bottom of the dispersion curve indicated in the figure by the dotted line (2), but it is still below the inflection point in the dispersion curve at 442 kHz.

The speed of these localized modes through the lattice is found to depend strongly on the driver amplitude, as seen in Fig. 3(b). Here, the speed measured in lattice constants a per ms (left axis) is plotted as a function of driver amplitude at a fixed frequency of 288 kHz. Thus the data points in Fig. 3(b) were collected by moving along the dashed line (1) in Fig. 3(a). It is evident that the speed increases fairly linearly with amplitude. The speed is also somewhat dependent on the driver frequency, but here the frequency shifts are much finer with lower frequencies giving rise to slightly faster ILMs. A similar dependence of ILM speed on amplitude and frequency of the driver is found within the 2 ILM region as well.

This speed dependence may seem somewhat counterintuitive, as larger driving is usually associated with sharper ILMs, and sharper ILMs are known to be less mobile. In this low-Q system, however, the ILM width is limited by the damping so that the ILM cannot become too narrow, and hence the barrier to translation cannot appear. Indeed, higher driving amplitudes do not seem to make the ILM significantly sharper. Instead, in this large damping regime, the driver amplitude changes the relative phase of the ILM with respect to the driver. As seen in Fig. 3(b) on the right axis, the phase relationship between the driving voltage and the response of the ILM center increases with amplitude, and it correlates with the velocity increase.

Let us now characterize the emergence of traveling ILMs more closely by examining the response when the driver is abruptly switched on. In the density plots of Fig. 4, the gray-scale indicates the energy, dark referring to higher energy. Energy at each node is computed by squaring the response voltage and then averaging over one period. The driving conditions corresponding to the panels of Fig. 4 are marked in Fig. 3(a) by the symbols "x." In Fig. 4(a), the driver is inside the lower hatched region (see lowest "x"). Here we see that after the driver is turned on, many localized features are launched in both directions. Out of this fluctuating state, the driver quickly selects and locks onto a particular traveling ILM. This ILM then persists indefinitely, as seen in the figure. In Fig. 4(b), the driver frequency is raised into the gap between the two hatched regions in Fig. 3(a). No single stable ILM emerges from the initial instability. Instead, the pattern of localization seems to switch between one and two

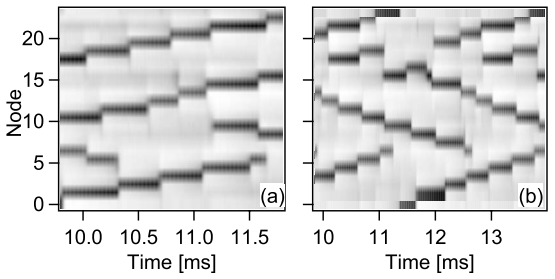

FIG. 5. Two stable patterns in the region between three and four ILMs. In (a), the driver frequency is 472 kHz, and in (b) 475 kHz. Both patterns are characterized by a switching between three and four simultaneous ILMs.

localized modes at any given time. In Fig. 4(c), the driver frequency is raised again and now falls within the 2ILM region. This time the system chooses the stable pattern of two ILMs traveling in tandem through the lattice.

In Fig. 4(d), the driver amplitude was lowered from 3.5 to 1.0 V. The frequency of 310 kHz was chosen to lie just below the uniform mode. Here the motion of the ILMs is not coherent but characterized by fairly random hops from site to site. Nevertheless, the driver does maintain this random walk without forcing the system into a coherent pattern. Interestingly, the three localized features produced by the initial modulational instability meander in unison for roughly the first 7 ms.

In order to test the effect of changing the ratio of inter- to on-site nonlinearity, we now replace the inductors to ground, changing L_2 from 330 to 150 μH. Thus the ratio decreases from 0.49 to 0.22. Besides raising ω_0, this change causes a drastic decrease in the speed of the propagating ILMs. For instance, at a driver amplitude of 2.5 V, the speed decreases from about 20 a/ms to anywhere between 3.5 to 1.9 a/ms, depending on the driver frequency and number of ILMs produced.

Furthermore, concurrent with the reduction in ILM speed is an increase in the number of ILMs comprising a stable driving pattern. We observe stable patterns involving between two and five ILMs as the driving frequency is increased. The driving regimes, in which these patterns characterized by different numbers of ILMs are stable, are again separated in frequency. One remarkable observation is that in between these regions stable patterns of localized features can also be found. Figure 5 illustrates the frequency region between three and four ILMs at a driver amplitude of 2.5 V.

In Fig. 5(a), the frequency is 472 kHz and in Fig. 5(b) it is raised to 475 kHz which is closer to the 4ILM region (starting at 481 kHz). Notice that in both panels, the pattern shifts back and forth between three and four ILMs in a repeatable fashion. At 472 kHz (left), we start out with four ILMs, the middle two close together initially. As time progresses, those two ILMs move apart, and one of them then merges with the lowest ILM. At this point, three ILMs remain. The middle of the three then travels at a somewhat larger speed, creating space for another ILM to be created later.

At 475 kHz, the pattern is a bit more complex. In Fig. 5(b), we start off with three ILMs. Since one ILM moves in the opposite direction, a gap opens up into which a forth ILM is created. Contrary to Fig. 5(a), here the pattern spends more time in the four ILM state than in the three ILM state, which is consistent with the larger driver frequency.

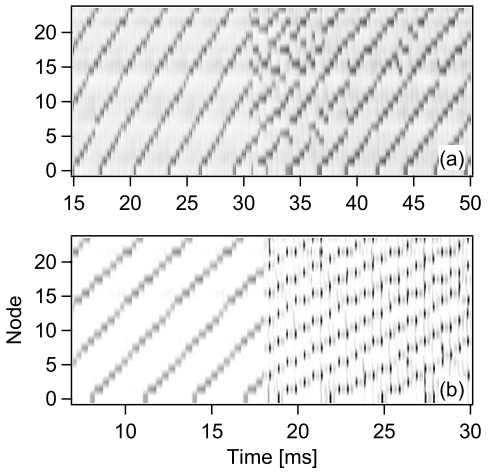

FIG. 6. The effect of abrupt frequency increases of the driver to investigate the transition from one ILM pattern to another. (a) Transition from a three to four ILM regime and (b) transition from a three to six ILM regime.

It is well-known that the transition from one pattern to another of different spatial periodicity is often facilitated by the emergence of defects [15]. In order to investigate the pattern selection process in this experimental system further, we made use of the FSK capabilities of the signal generator that provided the driving signal. More specifically, the driving frequency was first set to a value consistent with a particular number of ILMs, and then abruptly raised to produce a larger number of ILMs. The question is how one pattern that has become unstable due to the change in driving conditions gives way to another pattern.

Typical results are shown in Fig. 6; the driver amplitude is 2.5 V. In Fig. 6(a), the driver is abruptly changed at around 30 ms from 464 to 484 kHz. The former frequency is in the 3 ILM region and the latter in the 4 ILM region, and indeed these two patterns are observed at the beginning and the end of the graph. In the transition region, however, we see that defects play a pivotal role in transforming the pattern globally.

In Fig. 6(b), the driver again starts out at 464 kHz but is then increased to 502 kHz, which is consistent with 6 ILMs. Here the transition can happen more smoothly by simply inserting additional rows. Notice that the initial traveling ILMs can now continue undisturbed, albeit at a lower speed, and new ILMs are simply created in between.

IV. CONCLUSIONS

We have demonstrated that traveling ILMs can be generated in this nonlinear electrical lattice by a uniform driving signal. The speed of these localized modes is precisely tunable by adjusting the driver amplitude and frequency. Furthermore, the driver can excite and lock onto different numbers of ILMs propagating side by side depending on the

exact driving conditions. From a larger perspective, these ILMs should be understood in terms of the selection of driven patterns comprised of sharply localized features. In regions of phase space in which discrete wavelengths compete, more complex patterns can emerge for which the number of ILMs is not constant in time. By changing the driving frequency abruptly, we find that defects play an important role in the pattern selection mechanism.

ACKNOWLEDGMENTS

This research was supported by the Research Corporation. Discussions with Professor A. J. Sievers were very helpful.

[1] M. Remoissenet, *Waves Called Solitons*, 3rd ed. (Springer-Verlag, Berlin, 1999).
[2] R. S. MacKay and S. Aubry, Nonlinearity **7**, 1623 (1994).
[3] K. W. Sandusky, J. B. Page, and K. E. Schmidt, Phys. Rev. B **46**, 6161 (1992).
[4] D. Chen, S. Aubry, and G. P. Tsironis, Phys. Rev. Lett. **77**, 4776 (1996).
[5] S. Takeno and H. Kazunari, J. Phys. Soc. Jpn. **59**, 3037 (1990).
[6] S. R. Bickham, S. A. Kiselev, and A. J. Sievers, Phys. Rev. B **47**, 14206 (1993).
[7] S. R. Bickham, A. J. Sievers, and S. Takeno, Phys. Rev. B **45**, 10344 (1992).
[8] L. Q. English, M. Sato, and A. J. Sievers, Phys. Rev. B **67**, 024403 (2003).
[9] M. Sato and A. J. Sievers, Phys. Rev. Lett. **98**, 214101 (2007).
[10] R. Stearrett and L. Q. English, J. Phys. D **40**, 5394 (2007).
[11] P. Marquie, J. M. Bilbault, and M. Remoissenet, Phys. Rev. E **49**, 828 (1994).
[12] P. Marquie, J. M. Bilbault, and M. Remoissenet, Phys. Rev. E **51**, 6127 (1995).
[13] M. Sato *et al.*, EPL **80**, 30002 (2007).
[14] R. Basu Thakur, L. Q. English, and A. J. Sievers, J. Phys. D **41**, 015503 (2008).
[15] M. C. Cross and P. C. Hohenberg, Rev. Mod. Phys. **65**, 851 (1993).